

# Accepted manuscript doi: 10.1680/jgein.21.00027a

---

## **Accepted manuscript**

As a service to our authors and readers, we are putting peer-reviewed accepted manuscripts (AM) online, in the Ahead of Print section of each journal web page, shortly after acceptance.

## **Disclaimer**

The AM is yet to be copyedited and formatted in journal house style but can still be read and referenced by quoting its unique reference number, the digital object identifier (DOI). Once the AM has been typeset, an 'uncorrected proof' PDF will replace the 'accepted manuscript' PDF. These formatted articles may still be corrected by the authors. During the Production process, errors may be discovered which could affect the content, and all legal disclaimers that apply to the journal relate to these versions also.

## **Version of record**

The final edited article will be published in PDF and HTML and will contain all author corrections and is considered the version of record. Authors wishing to reference an article published Ahead of Print should quote its DOI. When an issue becomes available, queuing Ahead of Print articles will move to that issue's Table of Contents. When the article is published in a journal issue, the full reference should be cited in addition to the DOI.

# Accepted manuscript doi: 10.1680/jgein.21.00027a

---

**Submitted:** 09 June 2021

**Published online in ‘accepted manuscript’ format:** 09 November 2021

**Manuscript title:** Stress Crack Resistance of unaged High-Density Polyethylene  
Geomembrane Fusion Seams

**Authors:** W. Francey and R.K. Rowe

**Affiliation:** GeoEngineering Centre at Queen’s – RMC, Department of Civil Engineering,  
Queen’s University, Kingston, Canada

**Corresponding author:** R.K. Rowe, GeoEngineering Centre at Queen’s – RMC, Department  
of Civil Engineering, Queen’s University, Kingston, Canada, K7L 3N6.

**E-mail:** [kerry.rowe@queensu.ca](mailto:kerry.rowe@queensu.ca)

## **Abstract**

The stress crack resistance (SCR) of high density polyethylene (HDPE) geomembrane (GMB) fusion seams is examined for two 1.5mm HDPE GMBs and a range of welding parameters. Results are reported for both unnotched and notched seams as well as their corresponding sheet material. Unnotched seam SCR specimens are shown to preferentially initiate craze formation at the terminating edge of the squeeze-out bead, while incorporating potentially degraded areas, such as the seams heat-affected zone (HAZ), within the slow crack growth region of the specimen. In the short-term, little variation was observed between the majority of seams for the 9 welding parameter combinations examined, with an average normalized seam SCR value (normalized with respect to the unnotched sheet SCR) of  $0.3 \pm 0.1$ , or about 30% of the SCR of the unnotched sheet. It is shown that squeeze-out geometry plays an important roll in the SCR of fusion seams. Seams with weld track rippling, a known qualitative indication of overheating, were found to have average unnotched SCR values 45% lower than smooth weld track seams. Deleterious squeeze-out geometries are identified to provide a framework through which CQA engineers and researchers can more readily identify “higher risk” seams with respect to stress cracking.

**Keywords:** Geosynthetics, seams, welds, stress cracking resistance, HDPE, geomembranes, quality assurance

## 1. Introduction

High density polyethylene (HDPE) geomembranes (GMBs) are used extensively for the containment of fluids (Bouazza and Van Impe 1998; Rowe 1998, Hsuan and Koerner 1998; Thiel and Smith 2004; Hornsey et al. 2010; Jafari et al. 2014; Abdelaal et al. 2019; Abdelaal and Rowe 2019; Di Battista and Rowe 2020; McWatters et al. 2020; Morsy and Rowe 2020; Eldesouky and Brachman 2020; Yu and Rowe 2020; Li et al. 2021; Fan and Rowe 2021; Morsy et al. 2021; Rowe and Jabin 2021; Tuomela et al. 2021; Rowe and Fan 2021). Design-lives may range from decades to centuries depending on the materials used, temperature, fluid to be contained, and the degree of stress/strain to which the geomembrane barrier is subjected (McWatters et al. 2020; Rowe et al. 2019; Rowe 2020; Rowe et al. 2020; Yu and Rowe 2020). When subjected to sustained tensile loads or strains, and in particular those that do not cause short-term puncture, the HDPE geomembrane service life is controlled by the stress crack resistance (SCR) of the material (Peggs et al. 1990; Peggs and Carlson 1990; Hsuan 2000; Halse et al. 1990; Seeger and Muller 2003; Rowe et al. 2004; Peggs et al. 2014). Previous work has focused on the SCR of geomembrane sheet and selection of a sheet strain criterion for which to limit in field strains, such as those created by gravel indentations, at or below acceptable limits to avoid premature brittle failure (Seeger and Muller 2003 ; Abdelaal et al. 2014; Ewais et al. 2014c; Rowe et al. 2019; Rowe and Yu 2019;). While other studies have focused on the long-term SCR performance of GMB sheet immersed in synthetic solutions at elevated temperatures, such as synthetic landfill leachate or mining solutions (Abdelaal et al. 2014b; Ewais and Rowe 2014; Rowe et al. 2019; Rowe et al. 2009). Presently, limited studies have examined long-term HDPE GMB seam performance using oven jar immersion, with no studies having explored seam behaviour through performance testing and the use of geosynthetic liner longevity simulators (GLLSs). Prior to an examination of seam SCR with time, be it long-term jar immersion or GLLS, an in-depth

examination into the post-seaming SCR performance of HDPE GMB seams is required. The validation of a useful testing metric, comparison between sheet and seam failure times, and identification of welding parameters or seam geometries with deleterious effects on SCR performance will prove invaluable for both engineers and researchers in the identification of seams with a higher stress cracking risk in field, as well as aid in future examinations into the long-term performance of HDPE GMB seams.

There are limited studies examining the SCR performance, or more general performance such as tensile strength or standard oxidative induction time (Std-OIT) of HDPE GMB seams. Although, some work has identified seams as the weak point in an HDPE barrier system. Hsuan (2000) compiled a database of field incidents to examine both rapid and slow crack propagation failures at sixteen field sites in the United States of America, Canada, and one site in Italy. Of the sixteen failures, twelve experienced cracking at the location of the seam, with the majority of seam cracking failures occurring on the lower sheet directly adjacent to the seam itself. Moreover, six of the cracking failures were suggested to be the result of high welding temperatures or overheating during seaming, suggesting that material embrittlement can occur at this location if excessive heat is applied to the seam during welding. Often the cause of stress resulting in both these slow and rapid cracking failures was the result of thermal contraction, with twelve of the sixteen sites having noted the cause of the applied stress being 'thermal'. The effects of thermal contraction on cracking failures have been noted by others as well (Peggs et al. 1990; Peggs et al. 2014), with both fusion seams, and in particular extrusion seams, acting at the point of weakness for crack initiation. Peggs and Carlson (1990) suggested five features which require attention during GMB installation to mitigate cracking failures; thermal contraction stresses, residual stresses in seams, mechanical damage to the geomembrane or seams, creases/folds and notched

geometries in seams, and the synergistic effects of the exposure chemical and the stresses to which the GMB is subjected. This study also identified crazes along the outside edge of both fusion and extrusion seams where the parent sheet material intersects with the extrudate or squeeze-out bead. Peggs and Carlson (1990b) examined the single point notched constant tensile load (SP-NCTL) failure times and crack growth distances in GMB sheet and seams made from four different HDPE GMBs. It was concluded that in the majority of cases seaming processes increased the rate of crack growth through the sample as well as reduced SP-NCTL failure times when compared to sheet. Although they only examined a limited number of seams with unknown welding parameter combinations, the difference between seam and sheet appear to be greatest for extrusion welds compared to fusion welds, and even greater for seams produced using textured GMBs. The increased crack growth rates and decreased failure times were attributed to a sudden material density and crystallinity change experienced along the transverse direction of the seam (i.e., perpendicular to the seam direction), with the actual crack initiation location at the start of the density transition, rather than where peak material density values were measured. Halse et al. (1990) examined the failure surfaces of SP-NCTL HDPE GMB seam specimens, with the primary focus being to identify and describe the morphology of the fracture surfaces resulting from brittle detachment. It was concluded that, of the five identified morphological surface categories, that low to moderate applied stress levels resulted primarily in slow crack growth through a craze within the specimen, with higher stress levels resulting in failure surfaces more closely resembling that of fast impact fractures. In lower stress conditions, short fibrous and long fibrous morphologies were characteristic of slow crack growth within the sample.

Giroud et al. (1995) proposed a theoretical analysis for assessing the strain concentration occurring from welding two out of plane sheets and subsequent seam rotation when subjected to tensile stress. Kavazanjian et al. (2017) examined this phenomena experimentally and reported that the ratio between the maximum strains adjacent to the seam and the average specimen strain can range between 2.3 and 4.0, with peak strains reaching levels 1.4 to 2.0 times higher than that theorized by Giroud et al. (1995). Accelerated aging studies examining the long-term performance of HDPE fusion seams found that the heat-affected zone (HAZ), or area adjacent to the seam with the same thickness as the parent sheet, experienced faster OIT depletion and decrease in tensile break elongation depletion with time (Rowe and Shoaib 2017; Rowe and Shoaib 2018). While these studies identified the seam as a long-term potential weakness due to faster degradation, they only examined one seam with unknown welding parameters and did not examine the seam SCR performance with time raising the question as to what is the effect of the welding parameters on SCR. Zhang et al. (2017) examined three seams created using high heat, standard, and low heat applied welding parameters for the effect of these specific welding parameters on post-seaming antioxidant depletion. The HAZ in this study, much like that in similar studies (Rowe and Francey 2018; Rowe and Shoaib 2017), only experienced a small reduction in Std-OIT compared to the sheet on pre-aged HDPE seams. However, Zhang et al. (2017) identified the squeeze-out bead of a high heat-applied seam that showed irregular thermograms and the potential for significant Std-OIT depletion, suggesting this area may be more susceptible to degradation with time. Although, changes in seam SCR were not examined following this OIT depletion. The objective of this study is to fill some of the gaps identified above by

1. examining the suitability of available testing metrics for assessing seam SCR performance;

2. exploring the differences in SCR behaviour, both failure time and fracture surface morphology, between seam SCR samples created using different welding parameters and seams that exhibit known qualitative signs of overheating; and
3. identifying potential seam characteristics that adversely affect seam SCR performance.

## **2. Geomembranes examined**

Two 1.5mm HDPE GMBs, denoted MxA-15 and MwA-15, were examined (Table 1). MxA-15 is a 1.5 mm blown film HDPE GMB manufactured in 2008. Although it met the requirements GRI-GM13 at the time of manufacture and initial testing in 2008, as a result of the elapsed time in storage at room temperature, it had experienced partial antioxidant depletion yielding a Std-OIT of  $85 \pm 2$ min and HP-OIT of  $260 \pm 10$ min. The antioxidant package for MxA-15 did not contain hindered amine light stabilizers (HALS) (Ewais et al. 2014b; Abdelaal and Rowe 2015). Seaming of this material is analogous to seaming an extension onto an existing liner system, or the use of an GMB that has been stored for about a decade. This product may also serve as an analog for older geomembrane products used in installations that occurred before the use of more complex additive packages and base resins were employed in industry. MwA-15 is a more modern 1.5 HDPE flat die geomembrane manufactured in 2011 with a Std-OIT<sub>o</sub> of  $165 \pm 2$ min and HP-OIT<sub>o</sub> of  $1320 \pm 12$ min; both greater than GRI GM-13 requirements of 100min and 400min, respectively. Both geomembranes have sheet SCR<sub>o</sub> values (as determined by ASTM D5397) greater than 500 hours with MxA-15 being  $530 \pm 85$  hours and MwA-15 being  $1080 \pm 83$  hours.

### 3. Seaming Procedure

Fusion seams were created at three different sheet temperatures at the time of welding: 65°C, 21°C, and -27°C. Welding was conducted using both DemTech ProWedge and Leister G7 series wedge welders by an experienced welding technician.

The 65°C seams were welded on site at Queen's University's Environmental Liner Test Site (QUELTS) north of Kingston Ontario (44.5°N) on a sunny day about one hour after the midday sun (ambient temperature 30°C). At this time the sheet temperature was in equilibrium with sun exposure conditions at 65°C. The newly welded sections were left exposed to allow gradual cooling under warm weather conditions before sampling about 3 hours after welding. Seams were then transported and stored in the laboratory at 21°C.

The 21°C seams were created in a laboratory environment with sheet that had been stored in the lab and equilibrated to room temperature. The -27°C seam were created in an environmental chamber set to -27°C ± 1 C. The sheets to be welded were left to equilibrate with ambient temperature conditions for 24 hours prior to seaming. Newly created seams were then left for a further 24 hours in a -27°C environment prior to being stored at room temperature.

The primary focus of welding speed and wedge temperature selection was to include both high heat-applied and ideal heat-applied cases for seaming at a sheet temperature of 65°C. To isolate the effect of sheet temperature at the time of seaming, the same wedge temperature and welding speed were used at all three sheet temperatures. High heat applied cases included a wedge temperature of 460°C and welding speed of 1.8m/min (the minimum speed, at the machines maximum wedge temperature, with which a seam could be produced without burn-out failure at a 65°C sheet temperature). The more ideal heat-applied welding speed and temperature combinations utilized wedge temperatures of 360°C and 400°C with welding

speeds of 2.5 m/min and 3.0 m/min, respectively. This was based on the recommended DVS 2225-3 wedge temperature range of 300°C - 420°C and a maximum welding speed of 2.5 m/min. Hence, the selection of a 360°C, 2.5m/min combination. The 400°C wedge temperature 3.0 m/min welding speed combination incorporated a welding speed beyond this range to account for the reduced heat-applied needed for welding flat die geomembranes (Scheirs 2009), particularly when welded at high sheet temperatures such as 65°C.

Once acclimated to laboratory temperature, seams were cut and prepared for tensile peel and shear testing (ASTM D6392) to assess their strength/ductility with respect to GRI-GM19 criteria. The welded sample was cut into ten 25.4 mm x 150 mm specimens for each welding parameter combination. All seams examined passed peel separation (<25%), peel strength (>398 N/25 mm), shear strength (>525 N/25 mm) and shear break elongation (>50%) criteria, indicating that these welds would be suitable for in-field use based on these typical metrics.

It is acknowledged that certain parameter combinations, such as a sheet temperature of -27°C, may not be considered ideal (e.g., by GRI-GM9) although seaming at or around this temperature is not uncommon in Canada. Thus, the seams at -27°C were produced to identify if there were any fundamental changes in the stress crack behaviour for seams created at such cold temperatures. Similarly, other specific parameter combinations considered suitable for some sheet temperatures may not be considered suitable in all sheet temperatures examined. However, all seams passed GRI GM-19 strength/ductility criteria that would be considered acceptable at a large number of installations in North America.

#### **4. SCR testing**

SCR test specimens were cut and notched in accordance with ASTM D5397 and GRI-GM5(c) for both notched sheet SCR<sub>o</sub> and notched and unnotched seam specimens, respectively. Notched and unnotched SCR tests on seams were performed by centering the

leading edge of the seam, or HAZ/squeeze-out area, within the centre parallel region of a standardized 60.0 mm by 12.7 mm SCR dumbbell specimen (Fig. 1). This allowed regions of squeeze-out to fall within the parallel region of the SCR specimen, permitting this area to influence the test where it would influence performance in the field. The notched seam and sheet samples were notched using a stainless-steel cutting blade and computer aided design (CAD) controlled notching machine. Despite the high degree of accuracy this notching machine provided (0.00254mm), notching seams proved difficult, as the variation in squeeze-out amount between seams made notching perpendicular to the opposing sheet face opposite the squeeze-out bead and HAZ difficult to do consistently.

GRI-GM5(c) does not specify a minimum tolerance for the location of the notch relative to the critical stress cracking zone (CRIT) at the squeeze-out, sheet, HAZ interface. The CRIT area (Fig. 2) is characterized as the point where squeeze-out bead adherence to the HAZ ends and the sheet material starts. Once squeeze-out pools on the outside edge of a seam it either solidifies prior to adherence to the sheet, forming a shape resembling a 'teardrop' in cross-section, or contains enough heat within itself to create a 'pseudo-weld' (referred to as adherence) with the adjacent HAZ. Referring to Fig. 2, when the upper sheet material is loaded in tension and the zone between points A and B of length L is not adhered to squeeze-out, failure will occur at point B. Similarly, if the zone between points A to C are not adhered, failure would occur at point C. If the lower sheet material is loaded in tension, and the length L between points C and D is adhered to the squeeze-out, then failure will occur at point D. In general, the greater the extent of squeeze-out adherence the further the CRIT location is from the weld zone.

The adherence discussed above can be somewhat inconsistent and determining the degree of bonding can be difficult, as air gaps between bonded squeeze-out and the HAZ may be present. Moreover, as the degree of squeeze-out can vary significantly between seams, so does the angle at which the opposing sheets connect at the weld zone, making it difficult to consistently notch perpendicular to the sheet face within this area (i.e. the notch may fall at an angle  $<90^\circ$  to that of sheet face). The amount of squeeze-out and its degree of adherence can change depending on the welding parameters, shifting the position of the CRIT relative to the weld zone. Due to this, notched SCR testing may not be the most suitable means for assessing a seams susceptibility to stress cracking, as the exact preferential failure location may be unknown prior to notching. However, both testing metrics were examined for suitability in this study.

### **5. Notched vs Unnotched Seam SCR**

Three different seams were examined to assess the difference between the notched and unnotched SCR failure times (Table 2). For the notched specimens, the failure surfaces indicated that cracking initiated at the notch and then propagated towards the opposing sheet face containing the HAZ (Fig. 3). This was attributed to the stress concentration at the notch terminus resulting in crack initiation preferentially occurring at this location. Consequently, any potential HAZ or CRIT within the specimen fell within the global plastic failure region and, as a result, SCR failure times failed to incorporate any influence this location might have on slow crack growth. Failure surfaces from unnotched samples suggested the crack initiation was consistently at the CRIT and extended perpendicular to the direction of the applied load towards the opposing sheet face. This allowed the HAZ to fall within the brittle detachment region of the specimen, thus, providing failure times that incorporate craze formation and crack propagation through potentially degraded material within this region. MxA-15 failure times for notched seams ( $596 \pm 113$  hrs) were similar to that of the sheet material ( $529 \pm 85$

hrs). MxA-15 failure times for unnotched seams ( $964 \pm 260$  hrs) for the same welding parameters examined was notably less than the unnotched sheet failure time ( $>5300$  hrs), suggesting that the stress concentration at the notch terminus in notched specimens greatly affects the rate of slow crack growth within SCR specimens.

Due to variation in the extent of the squeeze-out and adherence, predicting the exact location of the CRIT for notched seam specimens proved difficult, potentially contributing to the relatively small difference between notched sheet and notched seam specimen failure time, as well as the slightly higher variation among notched seam specimens (compared to SCR<sub>o</sub> variation). The exact location of the most probable failure surface may be unknown prior to testing, but the process of notching requires one to predetermine the notch location, and ultimately the point of failure. Unnotched seam SCR specimens exhibited a preferential failure location at the CRIT, and as such, notched seam SCR testing should position the notch on the geomembrane sheet face opposite the CRIT location. Although, care must be taken into identifying the exact location of the CRIT based on the extent and degree of adherence of the squeeze-out bead. However, in order to include the HAZ and CRIT within the brittle detachment region, and for the purpose of a more direct comparison between seams and sheet (notably one which incorporates craze and crack formation time) this study focuses primarily on unnotched seam SCR values.

Unnotched seam SCR tests, rather than notched seam SCR tests, obtain seam SCR failure more representative of field seam performance. This is due to cracking initiating and propagating from the CRIT location through potentially degraded material in the HAZ, while notched seam SCR failure times fail to include the effect the HAZ has on SCR failure times. Testing seams in this method can provide engineers, CQA personnel and researchers a means through which the performance of a seam, relative to sheet material or other seams, can be

expected in the field. In particular, this test may be conducted when the SCR susceptibility of a HDPE fusion seam is in question following an installation or observed brittle failure in field.

## 6. SCR Performance

The averaged unnotched SCR failure times (Table 3) for the nine combinations of welding parameters (seaming sheet temperatures, welding speed, and wedge temperatures) were  $1220 \pm 300$  hours for MxA-15 and  $2580 \pm 1120$  hours for MwA-15 ( $n=27$  for each material). The ~2-fold higher average unnotched seam SCR value for MwA-15 can be largely attributed to the higher  $SCR_o$  of the sheet material, which is ~2-fold higher than that of MxA-15. Normalizing each seams average unnotched SCR to their corresponding notched sheet  $SCR_o$  value gave very similar normalized values of  $2.4 \pm 1.0$  for MwA-15 and  $2.3 \pm 0.6$  for MxA-15. Thus, for the range of parameters examined, it appeared that the two quite different geomembranes performed similarly with respect to post-seaming slow crack growth susceptibility.

Combining both normalized data sets, the average unnotched SCR value for all seams (Fig. 4;  $n=54$ ) was 2.4 ( $\pm 0.8$ )-fold greater than that of the ASTM D5379 notched sheet  $SCR_o$  value with the 95% two tailed confidence interval for the population mean falling between 2.1 and 2.6. Normalizing unnotched weld stress crack resistance with respect to the notched sheet  $SCR_o$  is simply a convenient way of accounting for the difference in stress crack resistance of the resin. The fact that the unnotched weld SCR averages more than twice the notched sheet  $SCR_o$  does not mean that the sheet is more susceptible to stress cracking than dual track fusion seams. The presence of the notch in notched sheet specimens serves as both an initiation location for a crack to propagate from as well as a point of stress concentration. This is evident through crack initiation location and propagation direction on notched seam

samples (Fig. 3). Moreover, the stress field within a notched and unnotched welded specimens is fundamentally different, making a direct comparison of these index test's failure times difficult in terms of relative performance.

In lieu of this, unnotched sheet samples that exclude a controlled crack initiation zone (i.e., a notch) were performed to allow a more direct comparison between seam and sheet. Three unnotched sheet SCR specimens tested at 30% yield strength for their corresponding cross-sectional area were conducted for the MwA-15 material. Unnotched MwA-15 sheet failure times averaged 9600 hrs with corresponding maximum and minimum values of 12,122 and 8,275 hours, respectively (n=3). Despite both unnotched sheet and notched sheet samples both being subjected to tensile load equal to 30% of the yield strength, failure times varied significantly between the two. This is hypothesized to be the result of stress concentration at the notch location on notched specimens, the absence of a craze or well-defined crack initiation location (i.e., a notch) for unnotched specimens. Given that both unnotched seam and unnotched sheet specimens more closely resemble each other in terms of these conditions, the ratio between unnotched seam failure time and unnotched sheet failure time is considered a more accurate representation of the relative difference between sheet and seam. MxA-15 and MwA-15 seams were found to be  $<0.3$  (i.e.  $<30\%$ ) and  $0.3 \pm 0.1$  (i.e.  $30\% \pm 10\%$ ) of the unnotched sheet specimen's SCR, respectively. This difference in failure time highlights the increased SCR susceptibility of seams and helps explain why cracking failures in the field preferentially occur at seams rather than in the sheet (Halse et al. 1990; Hsuan 2000; Peggs and Carlson 1990; Scheirs 2009; Peggs et al. 2014).

Mean SCR failure times between seams of each material type were reasonably consistent for most seams, suggesting changes in welding speed, temperature, and sheet temperature at the time of welding had a limited effect on seam SCR, for the materials and parameter range

examined. Seam variability appeared highest among seamed sample parameter cases 3, 6, and 9. In particular, seam MwA#9, created using a  $-27^{\circ}\text{C}$  sheet temperature,  $350^{\circ}\text{C}$  wedge temperature, and a 2.5 m/min welding speed, exhibited an average failure time 0.6 times that of the notched sheet  $\text{SCR}_o$ , and  $< 0.1$  times that of the unnotched sheet value. Statistical analysis using a student t-test found a statistically significant difference between MwA#9 and the population mean (95% confidence).

Variation between seam SCR was hypothesized to be primarily the result of either, (1) overheating and oxidation of the polymer melt and subsequent squeeze-out while seaming, and/or (2) the geometry of the seam and position of squeeze-out on the outside face of the weld track affecting the stress conditions at the CRIT.

The weld parameter combinations with a high wedge temperature ( $460^{\circ}\text{C}$ ) and low welding speed (1.8 m/min) exhibited minimum specimen failure times for sheet temperatures of  $65^{\circ}\text{C}$  and  $21^{\circ}\text{C}$  that were 54% and 42% of the average weld failure time (1.3 and 1.0 times the notched sheet  $\text{SCR}_o$ ), for MxA#1 and MwA#4, respectively. This suggests that these conditions contributed to a reduction in SCR due to overheating and localized embrittlement, however the other geomembrane types with the same welding parameter combinations (MwA#1, and MxA#1) did not share a corresponding decrease in failure times, which suggests that seam overheating and localized embrittlement/morphological change within the HAZ either did not occur, or did not have a significant affect on SCR reduction. In contrast, the same combination of wedge temperature and welding speed for sheet temperature of  $-27^{\circ}\text{C}$  (MxA#7 and MwA#7) gave relatively high average seam SCR values, with minimum values that were 100% and 110% (rounded to two significant digits) of the average weld failure time (2.5 and 2.7 times the notched sheet  $\text{SCR}_o$ ), for MxA#7 and MwA#7, respectively. This suggest that the higher heat-applied wedge temperature and speed

combination had a limited and possibly beneficial effect on seam SCR when sheet temperature at the time of welding was  $-27^{\circ}\text{C}$ .

Lower heat-applied parameter combination #9 (wedge temperature  $352^{\circ}\text{C}$ , welding speed 2.5 m/min, sheet temperature  $-27^{\circ}\text{C}$ ) resulted in the smallest observed thickness reductions (0.11 and 0.14 mm for MxA#9 and MwA#9, respectively) and the greatest observed reduction in seam SCR failure times (minimum values 33% and 20% of the average weld failure time, and 80% and 50% of the notched sheet  $\text{SCR}_o$  for MxA#9 and MwA#9, respectively). However, no significant difference between MxA#9 and the population mean was found and variation between specimens was high. Conversely, MwA#9 exhibited little variation and resulted in a statistically significantly different (95% confidence) average failure time (25% the population average weld failure time and 60% of the notched sheet  $\text{SCR}_o$ ). Given the lower applied heat welding parameters used for this seam, this suggests that another factor may be controlling the relatively shorter failure time for the MwA#9 weld. For example, MwA#9's squeeze-out adhered to the geomembrane sheet or HAZ region. This squeeze-out adherence may have resulted in locked in stresses within the CRIT upon cooling and/or increased localized stress acting on or within the CRIT when subjected to a tensile load.

In addition to squeeze-out bead adherence, MwA#9 exhibited a discontinuity with its squeeze-out bead running parallel to the seam direction. This, in conjunction with squeeze-out adherence, allowed the transfer of load across the squeeze-out bead discontinuity when loaded in tension, ultimately becoming a location for craze initiation for this seam. Brittle detachment started within the discontinuity in the center of the squeeze-out bead and extended towards the opposing sheet face. Thus, this squeeze-out adherence and a discontinuity within the squeeze-out bead of this seam significantly reduced the unnotched

SCR failure time. In order to identify potential discontinuities such as this, one may need to destructively remove a portion of the seam and inspect the squeeze-out.

The discontinuity discussed above disappeared about 1.1m from the start of the welding track. Further down the length of the seam there was no discontinuity or adhered squeeze-out present. Unlike all other seams examined, which demonstrated consistent squeeze-out geometries within the welded seam, the disappearance of this squeeze-out discontinuity suggests that this seam may have required more time until welding machine equilibrium. This delay until machine equilibrium was not evident from any change in seam thickness reduction along the length of the seam, where sections of seam relatively close to the start of the weld track (<1.1m) exhibited the same, albeit small, thickness reduction of 0.14 mm as sections of seam closer to the end of the seam.

Although the welding speed and temperature settings for this seam are not considered ideal for this sheet temperature and the resulting thickness reduction was less than that required by the German DVS 2225-3 criteria (which is not commonly specified in North America), this seam was considered suitable based on its strength and ductility requirements usually specified in terms of peel and shear tests. Based on the significance of the squeeze-out discontinuity and its disappearance along the length of the weld track, these results suggest that it may be advantageous to leave panel lengths slightly longer than normal to account for a delay in time until equilibrium when seaming in sub-zero conditions. In particular, when tie-ins or the joining of slope to base panels in the liner system are expected to occur in conjunction with thermal contraction, one may benefit from having additional seam overlap prior to conducting the tie-in. This phenomenon may also partially explain, or at least provide insight, into any rapid cracking failure originating at a fusion seam near 'butt' or 'tie-in' seams of an HDPE barrier system.

## 7. Squeeze-out Geometry and Adherence

Increased sheet temperature at the time of welding for 65°C seams appeared to serve as a preheat mechanism encouraging adherence of the squeeze-out bead to the sheet material. One can draw parallels between this phenomenon and the preheating aspect of extrusion welding, where hot air is passed along overlapped, heat tacked, and surface ground sections of geomembrane to preheat the material prior to polymer bead adherence to its surface. It is hypothesized that solar preheating of the sheet to 65°C allowed the polymer melt, in the form of fusion seam squeeze-out, to adhere to the sheet surface more readily, resulting in an increased likelihood of squeeze-out adherence. Seam squeeze-out geometries for the welding parameter combinations examined (Fig. 5) fell into one of the three categories: 1) partial or inconsistent squeeze-out contact (e.g., MxA#1), 2) Fully adhered squeeze-out (e.g., MxA#2), or 3) fully detached squeeze-out (e.g., MxA#6). All seams exhibited squeeze-out to some degree, with the greatest amounts being found in seams created using higher heat-applied welding parameters and high sheet temperatures at the time of welding.

The most common shape of the squeeze-out was in the form of a “teardrop” shape. This is the result of molten polymer being forced from the weld zone of the seam and subsequently pooling outside the weld as the stress from the overlapping sheets is reduced (i.e., the stress forcing polymer outwards is greatest near the weld interface and reduces the further you are from the weld). If sheet temperature at the time of seaming was great enough, or enough heat was transferred to the underlying sheet during squeeze-out movement, then the force from the overlapping sheets, in addition to the weight of the squeeze-out bead itself, was in some cases sufficient enough to make squeeze-out adhere to the sheets HAZ. This was observed in seams MxA#1, MxA#2, MxA#3, MxA#4, MWA#1, MWA#2, MWA#3, MWA#4, MWA#7, and

MwA#9, where partial to complete squeeze-out adherence was observed to the bottom geomembrane sheet.

Partial squeeze-out adherence is characterized as a squeeze-out bead that is either lightly adhered to the adjacent geomembrane sheet or is adhered in such a way that air voids are present between portions of the squeeze-out bead sheet interface (Fig 5. MxA#1). In such a case, the squeeze-out bead can be easily dislodged from the bottom geomembrane sheet using a 'pick' test with a fingernail or knife edge. Seams MxA#1, MxA#4, MwA#1, MwA#2, and MwA#7 all exhibited partial rather than full adherence. Although appearing similar to seams that have fully adhered squeeze-out (i.e., cannot be separated via a 'pick' test), the squeeze-out bead will likely not carry load through the seam as it detaches from the underlying sheet during SCR testing or field loading. Analysis of the failure surfaces of both partially and fully adhered squeeze-out cases showed that failure occurred at the critical location (CRIT) and not within the squeeze-out bead itself (as happened for the MwA#9 seam). The CRIT was located at the edge of the weld when there was no adherence, and it moved outward with the outermost adhered point of the squeeze-out bead with partial or full adherence. Although a shift in failure location was noted, little difference was observed between the unnotched SCR values of these seams. Squeeze-out adherence, be it partial (MxA#1, MxA#4, MwA#1, MwA#2 and MwA#7 with a mean normalized SCR =  $2.4 \pm 0.4$ ) or complete (MxA#2, MxA#3, MwA#3 and MwA#4 with a mean normalized SCR =  $2.2 \pm 0.7$ ), did not significantly reduce the SCR of these seams, highlighting the significance of the MwA#9 discontinuity and its effect on seam failure time.

Squeeze-out adherence may not greatly affect the short-term unnotched seam SCR, however, these seams may prove more susceptible to SCR degradation with time given the potential antioxidant depletion and degradation potential of the squeeze-out (Zhang et al.

2017) and its ability to transfer load following full adherence. This issue needs further investigation.

Although no significant difference was observed between seams with full squeeze-out adherence and partial adherence, the SCR failure time of MwA#9 suggests that geometry and the presence of discontinuities within the squeeze-out bead play an important roll in the failure time of fusion seams. Given higher heat applied welding parameters and higher sheet temperatures at the time of welding increase the likelihood of squeeze-out adherence, allowing load to transfer through the squeeze-out bead and any potential discontinuities, it is recommended that welding parameters be selected to avoid adherence of the squeeze-out bead wherever possible. During seaming squeeze-out geometry can be inspected following destructive testing, and if adherence is noted, appropriate changes to the welding parameter combinations can be made to limit the degree of squeeze-out created, effectively reducing the likelihood of sufficient heat transfer from the squeeze-out to the sheet material and reducing the likelihood of adherence.

## **8. Morphology of brittle failure surfaces**

The failure surface morphology of unnotched seams was analyzed using both microscope and scanning electron microscope (SEM) imagery to: (1) confirm that the failure zone of the unnotched seam SCR specimens were indeed brittle, and (2) assess whether the morphology of crack surfaces matched those previously described in the literature (Halse et al. 1990). The framework provided by Halse et al. (1990) allows one to imply the stress conditions and the potential failure mode of seamed samples following brittle detachment during SCR testing. Fig. 6 illustrates the cracking progression as the crack extends through a seamed SCR specimen. Much like that described by Halse et al. (1990), craze formation starts at the squeeze-out, HAZ, weld zone interface (i.e., CRIT) and extends towards the opposing sheet

face. Section 'A' displays short to long-fibrous fracture structures and can be seen extending from this interface, indicating relatively low stress levels during this portion of the ligament cross-section. As this crack propagated through the sample, section 'B', shows a combination of intermittent ductile, long fibrous, and potential hackle structures transitioning towards final global plastic failure in section 'C' (Halse et al. 1990). These features on the failure surface were consistent for the majority of seams examined. The global plastic failure portion of the sample, although indicative of a more ductile failure type, is ubiquitous in both notched and unnotched seams and sheet alike. This is because as the crack extends through the material and the cross-sectional area is reduced, the increasing applied stress then leads to yielding and plastic failure on the remaining portion of the ligament. Even if brittle failure is observed within a SCR specimen, there will still be a portion of the sample which fails in a ductile manner. Where this behaviour may vary, or not be expected, was within very brittle SCR specimens, such as those that have been well aged or if the sheet has been excessively degraded and/or over-heated through seaming (Scheirs 2009). In specimens such as this, one may still observe a portion of the sample failing through global plastic failure but the proportion of detachment that occurs through this means may be less. The proportion of short to long-fibrous detachment, and progression to hackle structures with increasing stress, was consistent between all seams examined except for MwA-15#9. In this seam (Fig. 7), the squeeze-out discontinuity serving as a crack initiation location exhibited long-fibrous to flake structures within the HAZ/squeeze-out region of the failure surface, suggesting increased stress within the discontinuity or that the squeeze-out may have been sufficiently degraded during welding, aiding in craze formation through embrittlement. Although, crystallinity tests of the HAZ ( $56 \pm 2.2\%$ ,  $n=5$ ) for this seam suggest this material displays a crystallinity value similar to that of the sheet material ( $54 \pm 2.6\%$ ,  $n=5$ ), and that material embrittlement during

seaming or a crystallinity transition across this region was likely not the primary cause. Moreover, the pooling and adherence of the squeeze-out on top of the bottom geomembrane sheet would likely increase the effective cross-sectional area of the SCR sample, and an increase in stress resulting from regional thinning is unlikely. Instead, it is hypothesized that the discontinuity itself may have served as a potential zone for stress concentration, increasing the local stresses in that area and resulting in the observed failure surface and shortened failure time. Furthermore, adherence of this hot melt on the low temperature underlying sheet potentially resulted in the locking of stresses in the bottom geomembrane which may have assisted in brittle failure when subjected to tension. This increased stress, be it through a geometry based concentration within the squeeze-out discontinuity or the locking of stresses upon cooling of the melt, is considered to be the main cause of the observed difference in SCR failure between this specimen and the others observed.

The surface morphology of failed seam SCR specimens suggest brittle detachment and stress cracking occur at the CRIT location when slow crack growth is the predominant failure mechanism. Evidence from failure surface morphologies characteristic of higher stress brittle detachments suggest that squeeze-out geometry may lead to stress concentration, and ultimately shorter failure times in some seams compared to the population average observed in this paper. Increased stress in this region should be considered when conducting destructive testing through examination of the geometry and position of squeeze-out on HDPE fusion seams. Following identification of any potentially deleterious geometries, or if the stress cracking integrity of the seam is in question, unnotched SCR tests can be performed to assess the impact this geometry may have on the seam and if any subsequent actions, such as in-field repairs, should be implemented.

## 9. Qualitative Signs of Seam Overheating

Qualitative indications of seam overheating, such as weld track rippling (Fig. 8) or excessive thickness reduction and thinning at the weld zone, have been suggested as indicators of material embrittlement within the HAZ and increased susceptibility to stress cracking (Scheirs 2009). To examine these qualitative indications, and in particular the effect of weld track rippling, six seams were created using a different welding machine (Leister G7 wedge welder) utilizing a longer heating element of ~13cm, vs the ~9cm wedge length used in the creation of the previously examined seams. Seams were created using six different welding speeds, 9.0, 6.5, 5.2, 4.0, 3.6, and 3.2 m/min and the manufacturer recommended welding temperature of 400°C and seaming force of 1250 N. Due to the larger wedge length, this machine's manufacturer recommended seaming speed of 9.0 m/min (for a 1.5 mm HDPE GMB) is greater than that of the previously used welding machine. The goal of this parameter selection was to both identify the point at which rippling occurred within the weld track for the 21°C sheet temperature seams in terms of thickness reduction, as well as to use the manufacturers recommended temperature and pressure parameters to focus on the effect that changes in welding speed have on thickness reduction and subsequent stress cracking susceptibility.

Rippling occurred within the weld zone when welding speeds were  $\leq 4.0$  m/min and thickness reduction was  $\geq \sim 0.75$  mm, with ripple wavelength decreasing with further reductions in welding speed and subsequent increases in thickness reduction. SCR results suggests that, on average, welding speed induced rippling resulted in a SCR reduction of 2070 hours (from an average of 4650 hours unrippled to 2580 hours rippled; Fig. 9). This is attributed to the increase in squeeze-out and subsequent alteration of the stress conditions acting at the CRIT of rippled seams. However, analysis of the failure surface of two of the

three specimens tested at the lowest welding speed of 3.2 m/min found that specimen yielding, rather than brittle detachment, was the predominant failure mechanism. This was not consistent for all rippled weld zone seams, where all failure surfaces for seams created using welding speeds at or greater than 3.6 m/min exhibited brittle failure surfaces starting with short to long-fibrous progressing to global plastic failure (Fig. 6). This suggests that regional thinning or a change in stress conditions in high thickness reduction and squeeze-out amount seams may have increased localized stress leading to sample yielding. The mean unnotched SCR value for the six seams examined in this series resulted in a normalized SCR ( $3.4 \pm 1.4$ ;  $n=18$ ) greater than the aforementioned seams ( $2.4 \pm 0.8$ ;  $n=54$ ) created using the smaller wedge welder. Suggesting either differences in machine wedge size or applied seaming pressure may have influenced the relatively greater failure time for this series. Although, all seams tested from both wedge welders yielded seam SCR failure times significantly less than that of the unnotched sheet material (9,600 hrs with corresponding max and min values of 12,100 and 8,280 hours, respectively).

This research in indicates that seam rippling should be avoided in-field. This is consistent with what has previously been noted in the literature with respect to seam SCR and weld track rippling in the field (Scheirs 2009). CQA engineers should make note of any potential weld track rippling that has occurred, note the location and extent of rippling along the seam length, and have the welding parameters adjusted and the rippled seam repaired.

During seaming procedures, generally an increase in sheet temperature due to solar heating should be followed by an increase in welding speed an/or a decrease in wedge temperature to avoid any potential rippling due to overheating. Qualification welds, often performed twice a day (once in the morning and again in the afternoon), could also be conducted following a significant change in sheet temperature due to solar heating, allowing

one to identify the need for a change in welding parameters prior to continuing seaming following elevated sheet temperatures.

## 10. Summary and Practical Applications

Seam cracking susceptibility can be examined via both notched and unnotched SCR index test configurations, with the latter of which considered more suitable for a direct comparison between seams and sheet as the crack initiation location and direction of crack propagation incorporate potentially degraded material into the brittle detachment region of the test specimen. Furthermore, unnotched seam SCR specimens include craze formation times and exclude the stress concentration present around the notch in notched specimens, allowing crack initiation to occur within the CRIT rather than on the opposing sheet face/notch (Fig. 3).

Seam SCR was found to be reasonably consistent between the parameter combinations examined and exhibited average seam values proportional to the  $SCR_o$  of the sheet material. Indicating that higher  $SCR_o$  GMB sheet materials may exhibit greater SCR seams. This suggests that if seams are to be positioned within relatively high tensile stress areas within the barrier system, such as connections to rigid components like pipes or concrete structures, then the adoption of a higher  $SCR_o$  GMB will likely prove advantageous regarding seam cracking mitigation. For the materials, welding machines, and seaming parameters examined, and for GMB seams which pass GRI GM19 peel/shear criteria, unnotched seams exhibited a SCR value  $2.6 \pm 1.1$  (MwA-15 and MxA-15; n=72) times that of notched sheet  $SCR_o$  specimens and  $0.3 \pm 0.1$  (MwA-15; n=45) and  $< 0.3$  (MxA-15; n= 27) times that of unnotched sheet SCR specimens. Unnotched seam SCR specimens consistently displayed increased stress crack susceptibility when compared to the unnotched sheet. This is consistent with the literature, where both fusion and extrusion seams are known points of weakness within the

polymeric barrier system (Halse et al. 1990; Hsuan 2000; Peggs et al. 2014; Peggs and Carlson 1990; Peggs and Carlson 1990b; Scheirs 2009). This suggests that the observed relative performance of unnotched specimens may be more analogous to the expected performance in field than notched specimens. Also, the comparison between unnotched seam and notched sheet specimens suggest the increased stress at the notch terminus has a significant effect on the reduction of cracking failure times. This suggests that notches or gouges within the GMB (in the order of 20% nominal thickness) may be as, if not more, problematic than seams with respect to cracking susceptibility. However, given the extent of total seam length (e.g., over 78 km of fusion seams for a 50 ha landfill, assuming 6.8m wide by 170 m long GMB rolls) in an HDPE barrier system and the relative care taken to avoid large defects, the susceptibility of seams to stress cracking should not be overlooked. Moreover, stress concentration may result from smaller and more commonly overlooked defects such as surface scratches, although the extent to which they reduce a sheets unnotched SCR requires further investigation. Regardless, care should be taken in the field to avoid defects of any kind on the geomembrane.

Although average unnotched seam SCR values were greater than notched sheet SCR<sub>o</sub> values, a specific squeeze-out geometry was found to negatively influence seam SCR and yield failure times faster than the notched sheet SCR<sub>o</sub> (seam MwA#9). In this case, squeeze-out adherence and the presence of a discontinuity in the center of the squeeze-out bead running parallel to the seam direction resulted in the shortest observed seam SCR failure time. This was hypothesized to be the result of geometry induced stress concentration acting within the discontinuity and underlying sheet material and resulted in an average unnotched failure time of 660 hours compared to 9600 hours for the unnotched sheet, and an SCR<sub>o</sub> of 1080 hours for the notched sheet.

Squeeze-out geometry and adherence can play a notable role in seam stress crack susceptibility. The identification of potential “higher risk” squeeze-out geometries should be part of CQA procedures during geomembrane installation. Furthermore, from a failure forensics perspective, engineers who observe cracking failures extending from fusion welds should make note of the position and geometry of the squeeze-out bead at the weld where the crack was initiated, as this component of the seam may provide insight into the factors contributing to the observed failure.

Lastly, seams exhibiting weld track rippling but passing current GRI GM19 peel/shear strength/ductility criteria, resulted in a 45% reduction in SCR compared to non-rippled seams created using the same wedge welder.

## 11. Conclusions

This study examined the short-term SCR and behaviour of 18 distinct sets of dual wedge fusion seams created from two 1.5 mm-thick HDPE GMBs (MwA-15 a flat die GMB and MxA-15 a blown film GMB), all meeting GRI GM19 ductility criteria. The welds represent 9 distinct combinations of sheet temperature, wedge temperature, and welder speed for one commonly used wedge welder. A brief comparison was also made with welds made with a different welding machine. The results provide insight into the relative stress cracking susceptibility of seams and sheet material, as well the relative performance between seams produced with different welding parameters and materials. The results of this study have also shown that, for the GMBs, welding equipment, and conditions examined:

1. SCR testing of welds should be conducted on unnotched SCR specimens.
2. Specific welding parameter combinations using sheet temperature, welding speed, and wedge temperature variations from 65°C – (-27)°C, 1.8 - 3.0 m/min, and 360°C - 460°C, respectively, using a welder with a ~ 9 cm long wedge (DemTech Pro)

resulted in reasonably consistent *unnotched seam* SCR values corresponding to  $2.4 \pm 0.8$  ( $\pm$  one standard deviation) of the *notched sheet* ( $SCR_o$ ) for the 1.5 mm blown film and flat die geomembranes examined.

3. Specific welding parameter combinations using a sheet temperature of 21°C, wedge temperature of 400°C, and welding speed variations from 3.2 - 9.0 m/min, using a welder with a ~13 cm long wedge (Leister G7) resulted in *unnotched seam* SCR values corresponding to  $3.4 \pm 1.4$  ( $\pm$  one standard deviation) that of the *notched sheet* ( $SCR_o$ ) for the 1.5 mm flat die geomembrane examined. Highlighting that the choice of welding machine and welding parameters can have a notable effect on post-weld SCR.
4. Welds were points of weakness with an initial (unaged) *unnotched seam* SCR about 30% (range: 20-40%) of the value for *unnotched sheet* for both the blown film and flat die geomembranes examined.
5. The combination of a discontinuity in the squeeze-out in conjunction with squeeze-out adherence appeared to play an important roll in reducing *unnotched seam* SCR.
6. Weld track rippling resulted in a 45% reduction in *unnotched seam* SCR and should be avoided even if the seam passes current GRI GM19 ductility criteria.

This paper only dealt with the SCR of the welds shortly after welding. The effect of welding parameters on the reduction in SCR with aging requires further investigation.

### **Acknowledgments**

The research was funded by Strategic Grant STPGP521237 – 18 from the Natural Sciences and Engineering Research Council of Canada (NSERC). In-kind support was provided by Titan Environmental and Leister Technologies AG. Funding for the development of the research infrastructure was provided by the Canada Foundation for Innovation, the Ontario Innovation Trust, the Ontario Research Fund Award, and Queen's University under project 36663. The support of all those listed above is much appreciated; however, the opinions expressed in the paper are solely those of the authors.

## Notations

Basic SI units are given in parentheses.

SCR<sub>0</sub> Initial stress crack resistance of the sheet (s)

Std-OIT standard oxidative induction time (s)

HP-OIT high pressure oxidative induction time (s)

Abbreviations

HDPE high density polyethylene

GMB geomembrane

CRIT critical location for seam stress cracking

HAZ heat-affected zone of seam

SCR stress crack resistance

SP-NCTL single point notched constant tensile load

CQA construction quality assurance

## References

- Abdelaal, F., Rowe, R., & Brachman, R. (2014). Brittle rupture of an aged HDPE geomembrane at local gravel indentations under simulated field conditions, *Geosynthetics International*, 21(1): 1-23.
- Abdelaal, F. B., Rowe, R. K., & Islam, M. Z. (2014b). Effect of leachate composition on the long-term performance of a HDPE geomembrane, *Geotextiles and Geomembranes*, 42(4): 348-362.
- Abdelaal, F. B., & Rowe, R. K. (2015). Durability of three HDPE geomembranes immersed in different fluids at 85 C. *Journal of Geotechnical and Geoenvironmental Engineering*, 141(2): 04014106.
- Abdelaal, F., Morsy, M., & Rowe, R. K. (2019). Long-term performance of a HDPE geomembrane stabilized with HALS in chlorinated water, *Geotextiles and Geomembranes*, 47(6): 815-830.
- Abdelaal, F., & Rowe, R. (2019). Degradation of an HDPE geomembrane without HALS in chlorinated water, *Geosynthetics International*, 26(4): 354-370.
- ASTM D 3418. Standard test method for transition temperatures and enthalpies of fusion and crystallization of polymers by differential scanning calorimetry, American Society for Testing and Materials, West Conshohocken, Pennsylvania, USA.
- ASTM D 6392. Standard Test Method for Determining the Integrity of Nonreinforced Geomembrane Seams Produced Using Thermo-Fusion Methods, American Society for Testing and Materials, West Conshohocken, Pennsylvania, USA.
- ASTM D 3895. Standard test method for oxidative induction time of polyolefins by differential scanning calorimetry, American Society for Testing and Materials, West Conshohocken, Pennsylvania, USA.
- ASTM D 5885. "Standard test method for oxidative induction time of polyolefin geosynthetics by high-pressure differential scanning calorimetry." American Society for Testing and Materials D5885, West Conshohocken, Pennsylvania, USA.

- ASTM D 5397. Standard Test Method for evaluation of stress crack resistance of polyolefin Geomembranes Using Notched Constant Tensile Load Test, American Society for Testing and Materials, West Conshohocken, Pennsylvania, USA.
- Bouazza, A., & Van Impe, W. F. (1998). Liner design for waste disposal sites, *Environmental Geology*, 35(1): 41-54.
- Di Battista, V., & Rowe, R. K. (2020). TCE and PCE diffusion through five geomembranes including two coextruded with an EVOH layer, *Geotextiles and Geomembranes*, 48(5): 655-666.
- DVS 2225-3. (2016). Welding of lining membranes made of polyethylene(PE) for protection of groundwater, German Welding Society, Dusseldorf, Germany.
- DVS 2225-4. (2016). Welding of lining membranes made of polyethylene(PE) for the sealing of landfill and contaminated sites, German Welding Society, Dusseldorf, Germany.
- Eldesouky, H.M.G. and Brachman, R.W.I. (2020). "Viscoplastic modelling of HDPE geomembrane local stresses and strains". *Geotextiles and Geomembranes* 48(1): 41-51. [<https://doi.org/10.1016/j.geotextmem.2019.103503>].
- Ewais, A. M. R., & Rowe, R. K. (2014). Effect of aging on the stress crack resistance of an HDPE geomembrane, *Polymer Degradation and Stability*, 109: 194-208.
- Ewais, A. M. R., Rowe, R. K., & Scheirs, J. (2014b). Degradation behaviour of HDPE geomembranes with high and low initial high-pressure oxidative induction time, *Geotextiles and Geomembranes*, 42(2): 111-126.
- Ewais, A., Rowe, R. K., Brachman, R., & Arneppalli, D. (2014c). Service life of a high-density polyethylene geomembrane under simulated landfill conditions at 85 C, *Journal of Geotechnical and Geoenvironmental Engineering*, 140(11): 04014060.
- Fan, J-Y and Rowe, R.K., (2021) "Seepage through a Circular Geomembrane Hole when covered by Fine-Grained Tailings under Filter Incompatible Conditions" *Canadian Geotechnical Journal*, (in press). <http://dx.doi.org/10.1139/cgj-2020-0788>
- Giroud, J., Tisseau, B., Soderman, K., & Beech, J. (1995). Analysis of strain concentration next to geomembrane seams, *Geosynthetics International*, 2(6): 1049-1097.
- GRI-GM5(c). (1992). "Seam Constant Tensile Load (SCTL) Test for Polyolefin Geomembrane Seams, Geosynthetic Research Institute, Pennsylvania, USA.
- GRI-GM9. (2013). Cold Weather Seaming of Geomembranes, Geosynthetic Research Institute, Pennsylvania, USA.
- GRI-GM13. (2019). Standard specification for test methods, test properties, and testing frequency for high density polyethylene (HDPE) smooth and textured geomembranes, Geosynthetic Research Institute, Pennsylvania, USA.
- GRI-GM19. (2011). Seam Strength and Related Properties of Thermally Bonded Polyolefin Geomembranes, Geosynthetic Research Institute, Pennsylvania, USA.
- Halse, Y., Koerner, R., & Lord, A. (1990). Stress cracking morphology of polyethylene (PE) geomembrane seams, *Geosynthetics: Microstructure and Performance*, ASTM International.
- Hornsey, W. P., Scheirs, J., Gates, W.P., & Bouazza, A. (2010). The impact of mining solutions/liquors on geosynthetics, *Geotextiles and Geomembranes*, 28(2); 191-198

- Hsuan, Y. G., & Koerner, R. (1998). Antioxidant depletion lifetime in high density polyethylene geomembranes, *Geoenvironmental Engineering*, 124(6): 532-541.
- Hsuan, Y. G. (2000). Data base of field incidents used to establish HDPE geomembrane stress crack resistance specifications, *Geotextiles and Geomembranes*, 18(1): 1-22.
- Kavazanjian, E., Andresen, J., & Gutierrez, A. (2017). Experimental evaluation of HDPE geomembrane seam strain concentrations, *Geosynthetics International*, 24(4): 333-342.
- Jafari, N. H., Stark, T. D., & Rowe, R. K. (2014). Service Life of HDPE Geomembranes Subjected to Elevated Temperatures, *Hazardous, Toxic, and Radioactive Waste*, 18(1): 16-26.
- Li, C., Espinoza, D., & Morris, J. (2020). "Wind-induced uplift of exposed geomembrane covers: A proposed revision to conventional design approaches". *Geotextiles and Geomembranes*, 48(1), 24-31.
- Li, W., Xu, Y., Huang, Q., Liu, Y., & Liu, J. (2021). Antioxidant depletion patterns of high-density polyethylene geomembranes in landfills under different exposure conditions, *Waste Management*, 121: 365-372.
- McWatters, R., Jones, D., Rowe, R., & Markle, J. (2020). Investigation of a decommissioned landfill barrier system containing polychlorinated biphenyl (PCB) waste after 25 years in service, *Canadian Geotechnical Journal*, 57(6): 882-902.
- McWatters, R., Rowe, R., Di Battista, V., Sfiligoj, B., Wilkins, D., & Spedding, T. (2020). Exhumation and performance of an Antarctic composite barrier system after 4 years exposure, *Canadian Geotechnical Journal*, 57(8): 1130-1152.
- Morsy, M., & Rowe, R. K. (2020). Effect of texturing on the longevity of high-density polyethylene (HDPE) geomembranes in municipal solid waste landfills *Canadian Geotechnical Journal*, 57(1): 61-72.
- Morsy, M. S., Rowe, R. K., & Abdelaal, F. B. (2021). Longevity of 12 geomembranes in chlorinated water, *Canadian Geotechnical Journal*, 58(4): 479-495.
- Peggs, I. D., & Carlson, D. S. (1990). Brittle fracture in polyethylene geomembranes, *Geosynthetics: Microstructure and Performance*, ASTM International.
- Peggs, I. D., & Carlson, D. S. (1990b). The effects of seaming on the durability of adjacent polyethylene geomembranes, *Geosynthetic Testing for Waste Containment Applications*, ASTM International.
- Peggs, I. D., Carlson, D. S., & Peggs, S. J. (1990) Understanding and preventing 'shattering' failures of polyethylene geomembranes, *Proceedings of the Fourth International Conference on Geotextiles, Geomembranes and Related Products*, AA Balkema, Rotterdam, Netherlands, pp. 549-553.
- Peggs, I., Gassner, F., Scheirs, J., Tan, D., Arango, A., & Burkard, B. (2014). Is there a resurgence of stress cracking in HDPE geomembranes, *Proceedings of the 10th International Conference on Geosynthetics, Berlin, Germany*.
- Rowe, R.K. (1998). "Geosynthetics and the minimization of contaminant migration through barrier systems beneath solid waste", *Proceedings of the 6<sup>th</sup> International Conference on Geosynthetics*, Atlanta, pp. 27-103.

- Rowe, R. K. (2020). Protecting the Environment with Geosynthetics: 53rd Karl Terzaghi Lecture, *Journal of Geotechnical and Geoenvironmental Engineering*, 146(9): 04020081.
- Rowe, R. K., Abdelaal, F., Zafari, M., Morsy, M., & Priyanto, D. (2020). An approach to high-density polyethylene (HDPE) geomembrane selection for challenging design requirements, *Canadian Geotechnical Journal*, 57(10): 1550-1565.
- Rowe, R.K., and Fan, J-Y (2021) "Effect of Geomembrane Hole Geometry on Leakage Overlain by Saturated Tailings". *Geotextiles and Geomembranes* (in press)
- Rowe, R. K., & Francey, W. (2018). Effect of dual track wedge welding at 30°C ambient temperature on post-weld geomembrane oxidative induction time, *Proceedings of the 11th International Conference on Geosynthetics, Seoul, Korea*.
- Rowe, R.K. and Jabin, F. (2021) "Effect of prehydration, permeant, and desiccation on GCL/Geomembrane interface transmissivity ", *Geotextiles and Geomembranes*, (in press).
- Rowe, R. K., Morsy, M., & Ewais, A. (2019). Representative stress crack resistance of polyolefin geomembranes used in waste management, *Waste Management*, 100: 18-27.
- Rowe, R.K., Priyanto, D., & Poonan, R. (2019). Factors affecting the design life of HDPE geomembranes in an LLW disposal facility, *Proceedings of the WM2019 Conference, Phoenix, Arizona, USA*, pp. 3-7.
- Rowe, R. K., Quigley, R. M., Brachman, R. W., & Booker, J. R. (2004). *Barrier systems for waste disposal facilities*, Spon Press, London, UK.
- Rowe, R. K., Rimal, S., & Sangam, H. (2009). Ageing of HDPE geomembrane exposed to air, water and leachate at different temperatures, *Geotextiles and Geomembranes*, 27(2): 137-151.
- Rowe, R. K., & Shoaib, M. (2017). Long-term performance of high-density polyethylene (HDPE) geomembrane seams in municipal solid waste (MSW) leachate, *Canadian Geotechnical Journal*, 54(12): 1623-1636.
- Rowe, R. K., & Shoaib, M. (2018). Durability of HDPE geomembrane seams immersed in brine for three years *Journal of Geotechnical and Geoenvironmental Engineering*, 144(2): 04017114.
- Rowe, R. K., & Yu, Y. (2019). Magnitude and significance of tensile strains in geomembrane landfill liners, *Geotextiles and Geomembranes*, 47(3): 439-458.
- Scheirs, J. (2009). *A guide to polymeric geomembranes: a practical approach*, John Wiley & Sons, West Sussex, UK.
- Seeger, S., & Muller, W. (2003). Theoretical approach to designing protection: selecting a geomembrane strain criterion, *Proceedings of the 1st IGS UK Chapter National Geosynthetics Symposium held at The Nottingham Trent University on 17 June 2003*, Thomas Telford Publishing, pp. 137-151.
- Thiel, R., & Smith, M. E. (2004). State of the practice review of heap leach pad design issues, *Geotextiles and Geomembranes*, 22(6): 555-568.

- Tuomela, A., Ronkanen, A.-K., Rossi, P. M., Rauhala, A., Haapasalo, H., & Kujala, K. (2021). Using Geomembrane Liners to Reduce Seepage through the Base of Tailings Ponds—A Review and a Framework for Design Guidelines, *Geosciences*, 11(2); 93.
- Yu, Y., & Rowe, R. K. (2020). Geosynthetic liner integrity and stability analysis for a waste containment facility with a preferential slip plane within the liner system, *Geotextiles and Geomembranes*, 48(5); 634-646.
- Zhang, L., Bouazza, A., Rowe, R., & Scheirs, J. (2017). Effect of welding parameters on properties of HDPE geomembrane seams, *Geosynthetics International*, 24(4): 408-418.

Table 1. Index properties at the time of testing for the two geomembranes examined, MwA-15 and MxA-15.

Properties	Method	Unit	GMB1	GMB2
Nominal thickness	ASTM D 5199	mm	1.5	1.5
GMB designation			MwA-15	MxA-15
Manufacturing date			2011	2005
Manufacturing technique			Flat die	Blown film
Standard oxidative induction time (Std-OIT)	ASTM D 3895	min	165 ± 2	85 ± 2
High-pressure oxidative induction time (HP-OIT)	ASTM D 5885	min	1321 ± 12	260 ± 10
Suspected HALS			Yes	No
HLMI (21.6 kg/190 °C)	ASTM D 1238	g/10 min	21.5 ± 0.2	19.7 ± 0.4
SCR	ASTM D 5397	hours	1078 ± 83	529 ± 85
Yield stress for SCR		kN/m	29.3	30.8
Tensile yield strength (MD)	ASTM D 6693 Type (IV)	kN/m	29.6 ± 0.5	29.3 ± 0.8
Tensile yield strain (MD)		%	19.7 ± 0.3	19.4 ± 0.5
Tensile break strength (MD)		kN/m	46.4 ± 0.3	38.9 ± .12.9
Tensile break strain (MD)		%	760 ± 13.8	760 ± 84.0

Table 2. MxA-15 SCR failure times for notched and unnotched specimens. Seamed samples are normalized to their corresponding notched or unnotched sheet equivalent.

Material	Type	Notch	Sheet temp at time of weld	Welding Speed (m/min)	Welding Temp (°C)	Crack Initiation Location	Average Failure Time (hours)	Normalized average Failure time*	Maximum (hours)	Minimum (hours)
----------	------	-------	----------------------------	-----------------------	-------------------	---------------------------	------------------------------	----------------------------------	-----------------	-----------------

				ing (°C)							
MxA-15	Virgin Sheet	Notched	N/A	N/A	N/A	Notch	529	1.00	660	470	
	Weld		65	1.8	460		588	1.11	620	540	
			21	3	400		659	1.25	770	510	
			-27	2.5	350		540	1.02	640	380	
	Virgin Sheet	Unnotched	N/A	N/A	N/A	N/A	> 5300	1.00	N/A	N/A	
	Weld		65	1.8	460		CRIT	968	< 0.20	1180	690
			21	3	400			962	< 0.20	1010	920
			-27	2.5	350			964	< 0.20	1310	450

\*Normalized to notched or unnotched sheet equivalent.

Table 3. List of parameter combinations examined for both MxA-15 and MxA-15 seams and their corresponding average unnotched SCR failure times (rounded to 3 significant digits).

Parameter combination	Sheet Temperature during Welding (°C)	Wedge Temperature (°C)	Welding Speed (m/min)	MxA-15 SCR Failure Time		MwA-15 SCR Failure Time	
				Average (hours)	Range (hours)	Average (hours)	Range (hours)
1	65 ± 5	460	1.8	970	1180-689	2660	3050-2060
2	65 ± 5	400	3.0	1250	1370-1150	3010	3990-2100
3	65 ± 5	352	2.5	1650	1890-1530	1710	2500-1200
4	21 ± 1	460	1.8	1240	1360-1190	1990	2450-1120
5	21 ± 1	400	3.0	960	1010-921	2860	3790-1810
6	21 ± 1	352	2.5	1150	1360-1000	3970	4590-2930
7	-27 ± 1	460	1.8	1520	1690-1300	2900	2970-2860
8	-27 ± 1	400	3.0	1310	1430-1220	3480	4200-3000
9	-27 ± 1	352	2.5	960	1300	660	840-

					-449		550
Unnotched Sheet	N/A	N/A	N/A	>5300	N/A	9600	1212-8275
Notched Sheet	N/A	N/A	N/A	530	659-471	1080	1140-980

### Figure captions

- Figure 1. Orientation and position of the HAZ, CRIT and notch (if present) in seam SCR specimens. In notched specimens, the 20% nominal thickness notch was positioned on the opposing sheet face opposite the squeeze-out and CRIT.
- Figure 2. Cross-sectional view of a typical HDPE fusion seam containing a squeeze-out bead. The critical zone (CRIT) for stress cracking initiation occurs at the squeeze-out, sheet, HAZ interface location, and is the preferential failure point for unnotched specimens (see text for a full description).
- Figure 3. Direction of crack propagation (for a 21°C sheet temperature, 400°C wedge temperature, 3.0 m/min welding speed seam), relative to HAZ and CRIT position for unnotched and notched seams. Notched specimens failed to capture the true effect of the welding whereas unnotched captured the critical location (CRIT) including potentially degraded material within the brittle detachment zone of a SCR specimen.
- Figure 4. Variation in normalized unnotched seam SCR for MxA-15 and MWA-15. Error bars for individual parameter combinations represent max and min values for three replicates.
- Figure 5. Squeeze-out was found to adhere in three different ways for the seams examined: 1) partial or inconsistent contact, 2) fully adhered, determined through a “pick test”, on one or two sides, and 3) fully detached on both sides.
- Figure 6. Surface morphology of a seam SCR failure surface. Crack propagation begins with the formation of a craze in zone A, where short to long-fibrous fracture surfaces indicative of relatively lower stress levels can be found. Zone B is a transitional region where increasing stress leads to intermitted ductile, long-fibrous, and potential flake structures as the cross-sectional area of the specimen reduces following crack propagation. Lastly, zone C is the global plastic failure region, where the cross-section area remaining on the sample is too small that the applied load exceeds the yield strength of the material.
- Figure 7. Surface Morphology of MWA-15#9’s failure surface. Flake to long-fibrous surface morphologies were found within the squeeze-outs beads discontinuity after failure, suggesting increased localized stress contributing to this specimen’s reduction in failure time.
- Figure 8. Seam rippling, a qualitative sign of seam over-heating, occurs when heat applied to the seam reaches a level high enough to melt a significant portion of the sheets thickness, in-turn permanently deforming the weld as the nip rollers apply pressure and the welding machine propels itself forward.

Figure 9. Variation in SCR failure time for three welds exhibiting weld track rippling, and three welds exhibiting a smooth weld track. Welding speed induced rippling resulted in an average SCR reduction of 2071 hours when compared to smooth weld track samples (n=9 for each case).

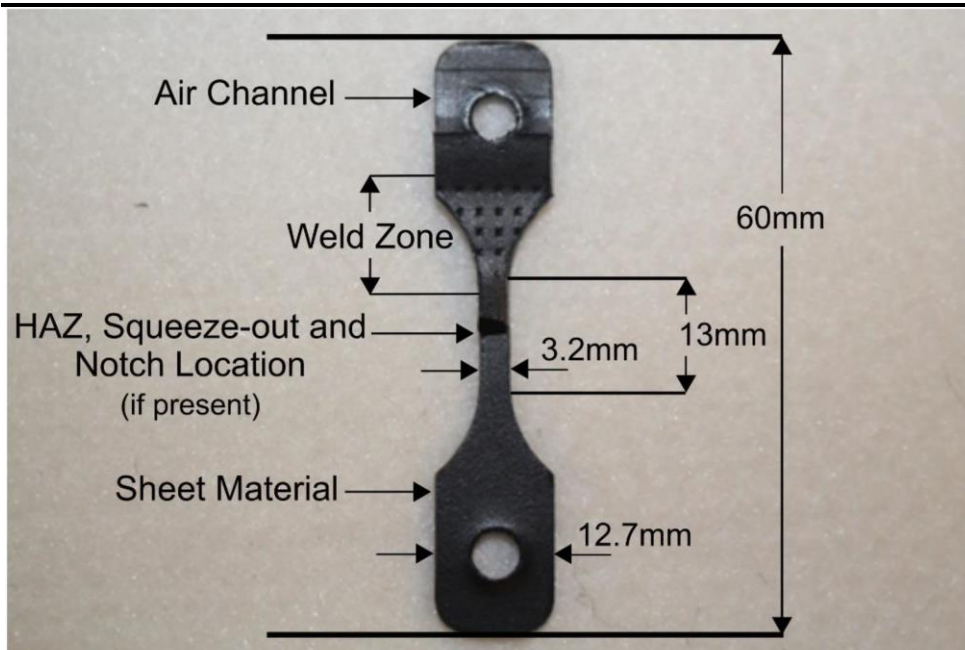


Figure 1

Stress cracking Critical Zone (CRIT) and changes in its  
position with degree of squeeze-out adherence.

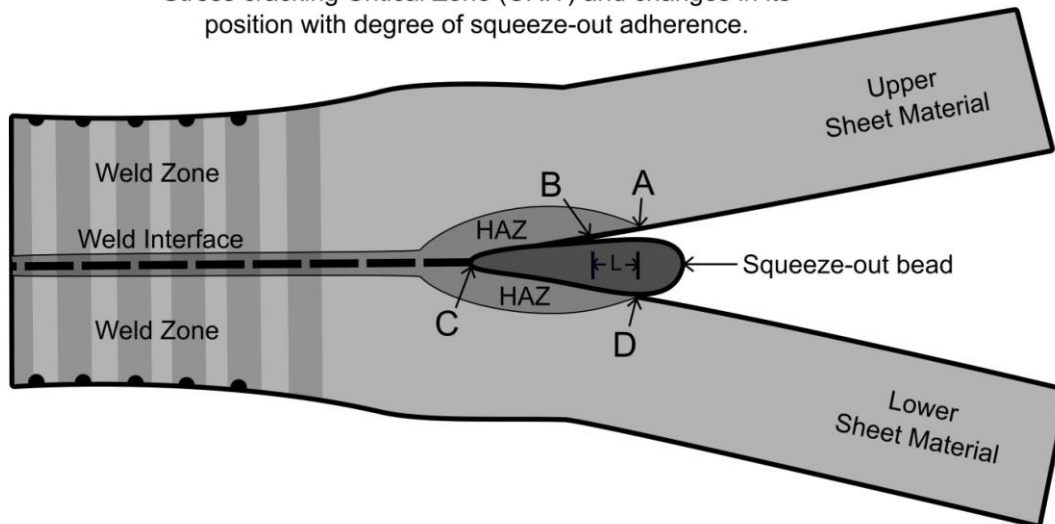


Figure 2

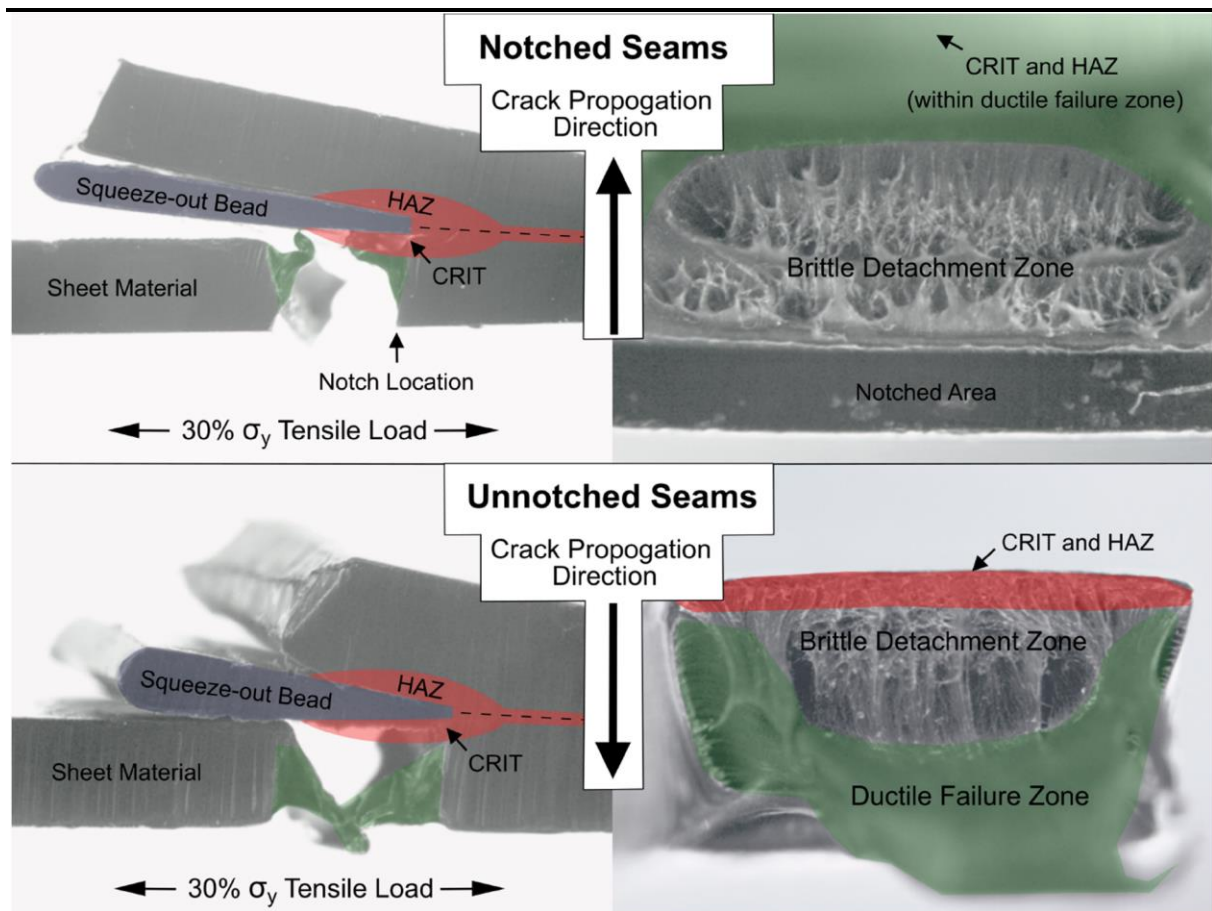


Figure 3

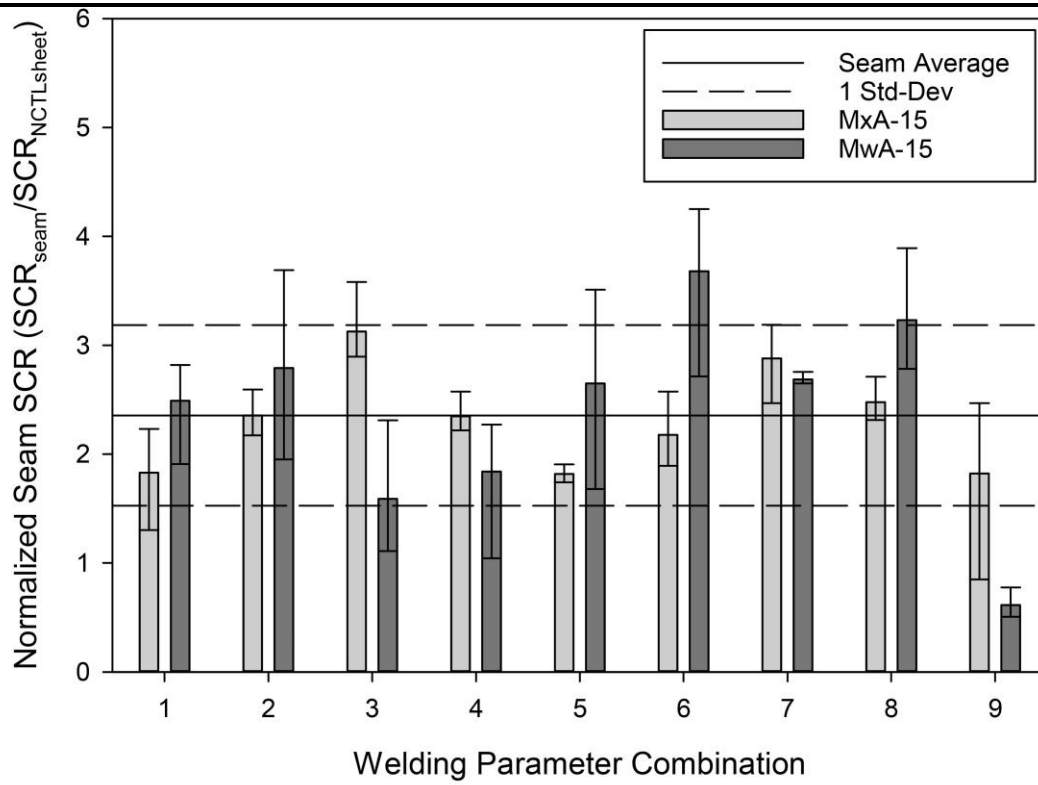


Figure 4

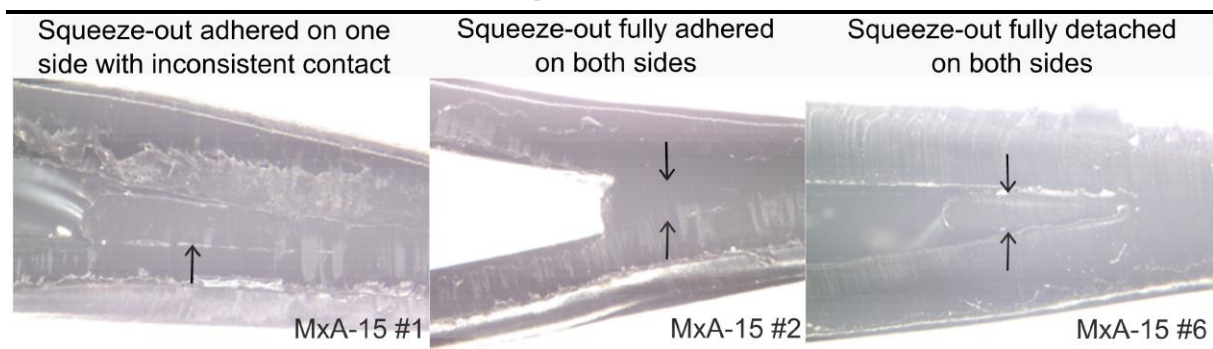


Figure 5

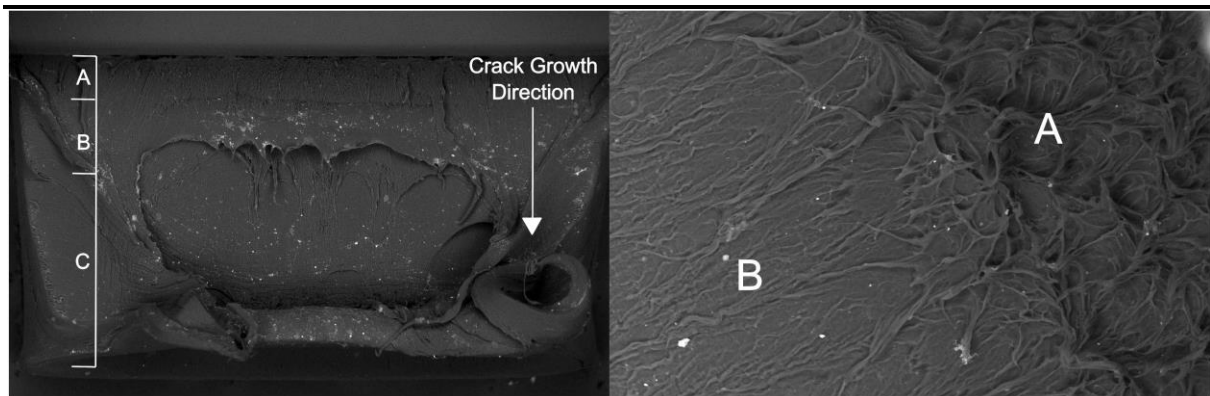


Figure 6

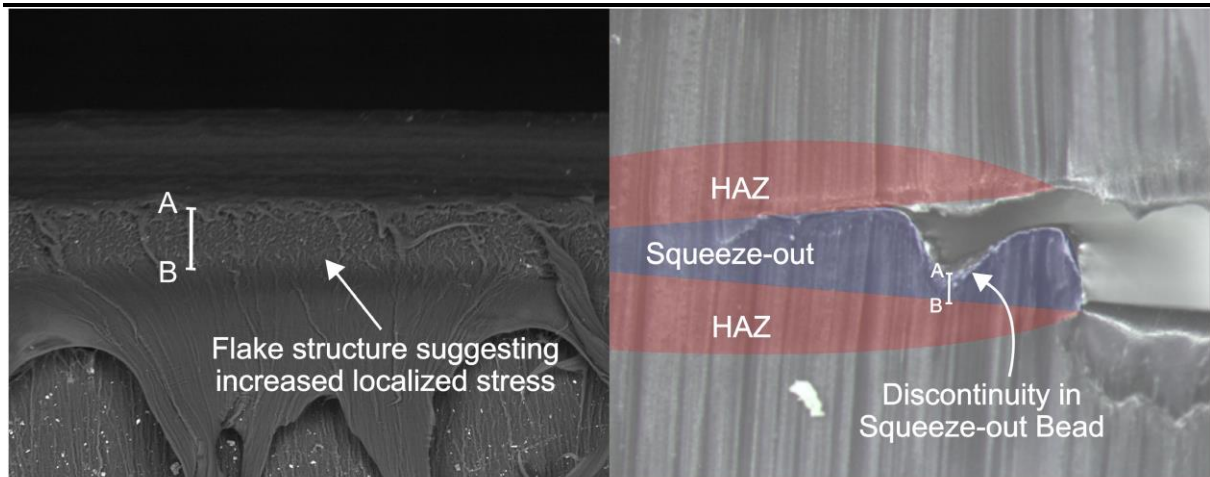


Figure 7

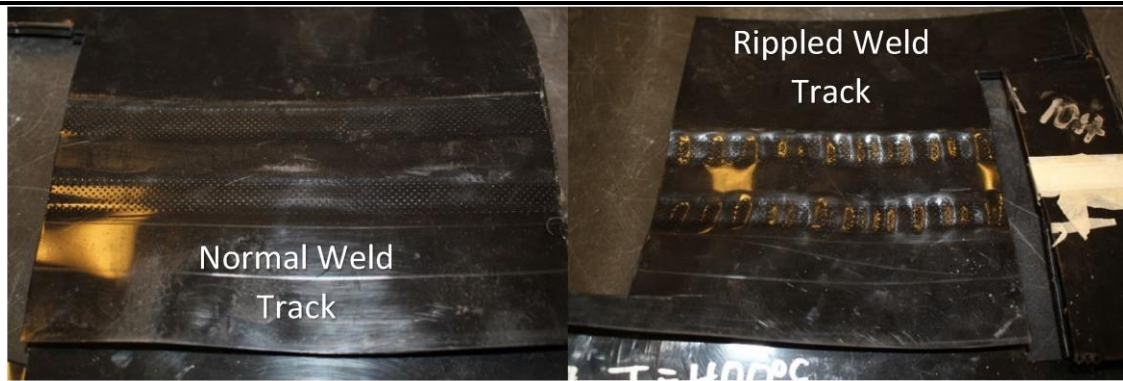


Figure 8

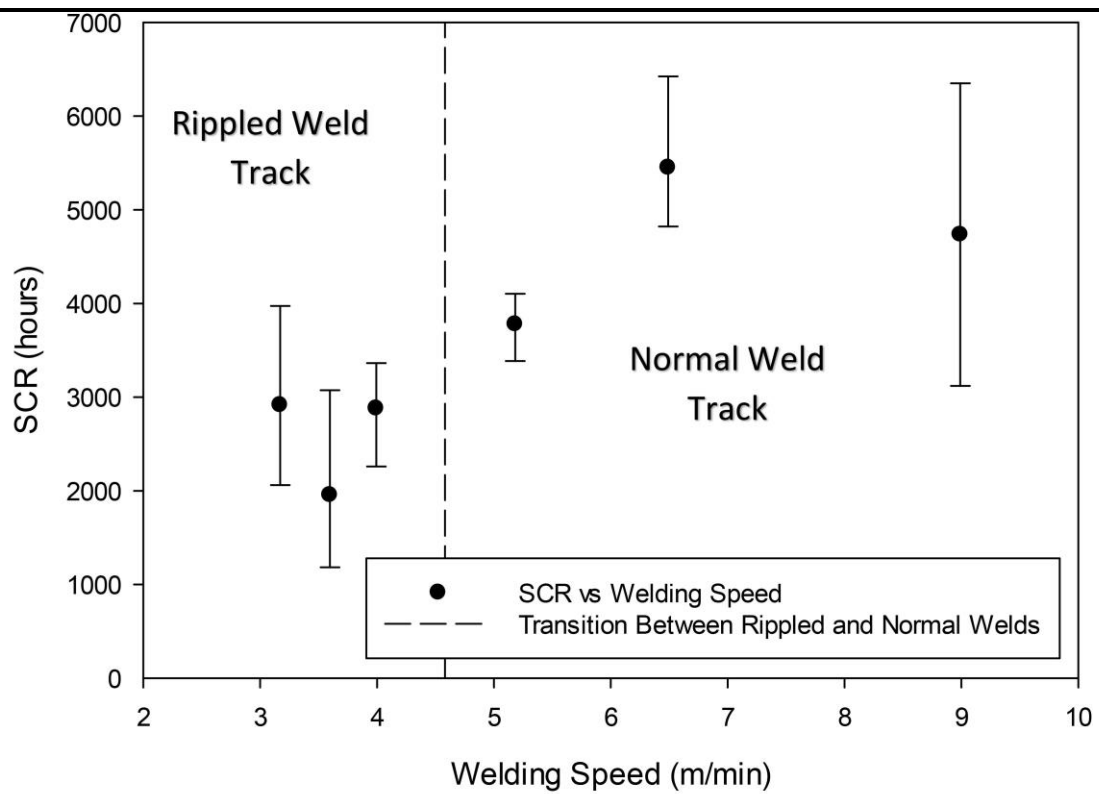


Figure 9